One-Electron-Transfer Reactions of Polychlorinated Ethylenes: Concerted and Stepwise Cleavages

Eric J. Bylaska* and Michel Dupuis

Pacific Northwest National Laboratory, P.O. Box 999, Richland, Washington 99352

Paul G. Tratnyek

OGI School of Science & Engineering, Oregon Health & Science University, 20000 NW Walker Road, Beaverton, Oregon 97006-8921

Received: November 19, 2007; In Final Form: February 6, 2008

Reaction barriers were calculated by using ab initio electronic structure methods for the reductive dechlorination of the polychlorinated ethylenes: C_2Cl_4, C_2HCl_3, *trans*-1,2-$C_2H_2Cl_2$, *cis*-1,2-$C_2H_2Cl_2$, 1,1-$C_2H_2Cl_2$ and C_2H_3-Cl. Concerted and stepwise cleavages of R−Cl bonds were considered. Stepwise cleavages yielded lower activation barriers than concerted cleavages for the reduction of C_2Cl_4, C_2HCl_3, and *trans*-1,2-$C_2H_2Cl_2$ for strong reducing agents. However, for typical ranges of reducing strength concerted cleavages were found to be favored. Both gas-phase and aqueous-phase calculations predicted C_2Cl_4 to have the lowest reaction barrier. Additionally, the reduction of C_2HCl_3 was predicted to show selectivity toward formation of *cis*-1,2-$C_2HCl_2^{\bullet}$ over the formation of *trans*-1,2-$C_2HCl_2^{\bullet}$, and 1,1-$C_2HCl_2^{\bullet}$ radicals.

I. Introduction

Some of the fundamental concepts that are central to our theoretical and mechanistic understanding of reactivity have also profound practical implications in environmental chemistry. These concepts include the distinction between inner- vs outer-sphere precursor complexes, electron vs atom transfer, and concerted vs stepwise bond cleavage. All three of these distinctions are relevant to reductive transformations of chlorinated aliphatic compounds such as carbon tetrachloride, 1,1,1-trichloroethane, and trichloroethylene, which are among the most common environmental contaminants due to their widespread use as solvents, degreasers, etc. The reduction of these compounds has been studied extensively, often in chemical or biomimetic model systems that allow fairly rigorous analysis and interpretation of the reduction of these chlorinated compounds.[1−9]

Hydrogenolysis, or reductive dechlorination, is a potential pathway for degradation of chlorinated ethylenes in any (more or less) anaerobic environment, including groundwater, sediments, wet soils, sludges, etc.[10] In this reaction, the addition of two electrons results in release of chloride and the formation of a new C−H bond on the chlorinated ethylene, i.e.

$$C_2H_xCl_{4-x} + 2e^- + H^+ \rightarrow C_2H_{x+1}Cl_{3-x} + Cl^- \qquad (1)$$

for $x = 0, 1, 2, 3$. Degradation may also occur by a reductive elimination reaction that involves two electrons and results in the release of two chloride ions and the formation of a triple C−C bond.

$$C_2H_xCl_{4-x} + 2e^- \rightarrow C_2H_xCl_{2-x} + 2Cl^- \qquad (2)$$

Both these dechlorination processes are assumed to occur in two sequential electron-transfer (ET) steps: the first electron transfer to the polychlorinated ethylene is a dissociative electron attachment reaction leading to the formation of a polychloroethylene-1-yl radical and a chloride ion.

$$C_2H_xCl_{4-x} + e^- \rightarrow C_2H_xCl_{3-x}^{\bullet} + Cl^- \qquad (3)$$

The second ET for the hydrogenolysis reaction allows the newly formed radical to bind to a proton to form a neutral compound,

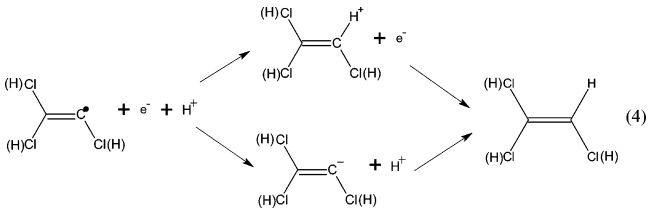

and the second ET for the elimination reaction results in the loss of another chloride and the formation of a triple C−C bond.

$$C_2H_xCl_{3-x}^{\bullet} + e^- \rightarrow C_2H_xCl_{2-x} + Cl^- \qquad (5)$$

It is believed that the rate-limiting step in both types of degradation reactions is the first ET (eq 3).[11] However, the details of this first ET step are not fully established. Two possible mechanisms have been identified for eq 3: a stepwise mechanism and a concerted mechanism.[11,12] In the stepwise mechanism a stable radical anion intermediate is formed which then subsequently undergoes dissociation. For the concerted mechanism, the ET and dissociation occur simultaneously. The distinction between these two mechanisms is illustrated in eq 6.

The electronic structure of the radical anion intermediate in the stepwise mechanism can be described as a 3-electron 2-orbital state of π character with carbon atoms that are sp^3 rather than sp^2 hybridized with a dangling lone pair of electrons on one carbon atom and an unpaired radical electron on the other carbon atom. Several experimental and computational

10.1021/jp711021d CCC: $40.75
Published on Web 03/27/2008

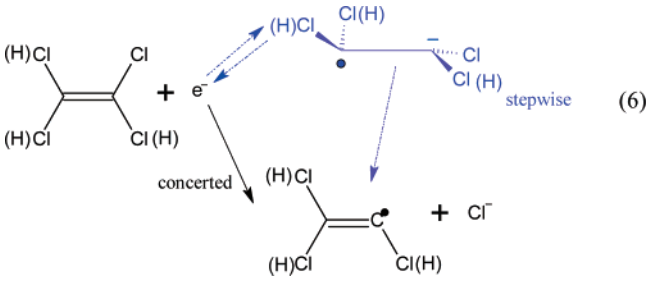

(6)

studies have confirmed the existence of such an intermediate for C_2Cl_4 in the gas phase.[13−20] However, for C_2HCl_3 and $C_2H_2Cl_2$ the existence of such an intermediate is less certain. Although thermal electron attachment negative ion mass spectrometry studies by Chen et al. suggest their existence,[14,20] similar studies by Johnson et al. do not,[16] and until recently[21] ab initio studies have failed to find a stable π^* radical anion for C_2HCl_3[22] and $C_2H_2Cl_2$. This is somewhat surprising because electron transmission spectroscopy studies[13,15,17,18] have unambiguously shown evidence for both Σ and Π anion resonance states, and that dissociative electron attachment usually proceeds through the Π anion resonance state.[19]

Which of the two reaction mechanisms shown in eq 6 is pertinent is in general not known for the chlorinated ethylenes, as it depends on factors including the degree of chlorination, the type of solvent, and the strength of the reductant.[11,23,24] However, recent cyclic voltammetry experiments in solution have supported the idea of the first ET to C_2Cl_4, C_2HCl_3, and $C_2H_2Cl_2$ proceeding via a stepwise mechanism.[11] In addition, a recent theoretical study in which the formation of the π^* radical anion was found to be nearly isoenergetic with other intermediate radical anions[21] has also buttressed the possibility of a stepwise mechanism.

Several groups have been interested in applying the methods of computational chemistry to study the environmental degradation of simple and larger organochlorine compounds.[2,21,22,25−41] In the present study, we extend a previous study in which we reported the thermochemical properties of chlorinated ethylenes,[21] to now provide estimates of the activation barrier as a function of the strength of the reducing agent for the concerted and stepwise reaction mechanisms for all the chlorinated ethylenes in the gas phase and in aqueous solution.

The computational methods used in this work are described in section II. Calculations for the activation barriers of the concerted and stepwise reaction pathways are reported in sections III and IV, respectively. The activation barriers are estimated using a strategy suggested by Saveant et al.[24,35,42] The barriers are determined by finding the crossing point between ab initio generated potential energy curves for the neutral species $C_2H_xCl_{4-x}$ and the radical anions $C_2H_xCl_{4-x}^{\bullet-}$ as a function of a reaction coordinate parameter (the C−Cl bond length). Concluding remarks are given in section V.

II. Ab Initio and Continuum Solvation Calculations

The ab initio calculations in this study were performed with Density Functional Theory (DFT)[43] and restricted open shell coupled-cluster calculations (RHF-RCCSD(T)).[44] The Kohn−Sham equations of DFT[45] were solved using the gradient corrected B3LYP[46,47] exchange-correlation functional using the 6-311++G(2d,2p) basis set.[48,49] The RHF-RCCSD(T) calculations used the aug-cc-pVTZ basis set.[50] The DFT calculations included most of the basis set ingredients (double polarization functions and diffuse functions) found in the RHF-RCCSD(T) calculations. This basis set, used in our earlier work,[21] is known

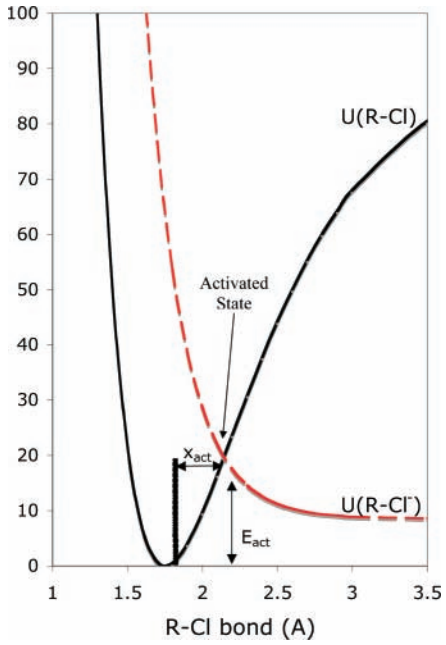

Figure 1. Illustration of curve crossing in dissociative electron attachment.

to be of near-quantitative accuracy set.[48,49] We note that the emphasis in the present investigation was not the comparison of results with different basis sets. Rather we used the RHF-RCCSD(T) method to critically assess the spurious effect of spin polarization in the description of the radical anion species. Most of the ab initio calculations in this study were performed with the NWChem program suite.[51] However, the MolPro program suite[52] was used to perform the RHF-RCCSD(T) calculations reported in section III.

In general, the solvation energies for rigid solutes that do not react strongly with water can be approximated as a sum of noncovalent electrostatic, cavitation, and dispersion energies.[53,54] In this study, the cavity and dispersion contributions were not calculated, because the activation energy calculations only needed the relative solvation energies between neutral and anionic species of the same structure. The electrostatic solvation energies were estimated using the self-consistent reaction field theory of Klamt and Schüürmann (COSMO),[55] with the cavity defined by a set of overlapping atomic spheres with radii suggested by Stefanovich and Truong (H 1.172 Å, C 1.635 Å, and Cl 1.750 Å).[56] The dielectric constant of water used for all of the solvation calculations was 78.4. This continuum model can be used with a variety of ab initio electronic structure methods in the NWChem program suite including DFT. Calculated gas-phase geometries were used to perform these calculations. The solvent cavity discretization was generated from the surface of overlapping spheres through an iterative refinement of triangles starting from a regular octahedron.[55] Three refinement levels, which is equivalent to 128 points per sphere, were used to define the solvent cavity in these calculations.

III. Activation Barriers for Concerted Reaction Pathways

The activation energy of a concerted ET reaction of chlorinated ethylenes (eq 3) is estimated by finding the crossing point, (x_{act}, E_{act}), between the dissociation potential energy curves for the neutral R−Cl species ($U_{C_2H_xCl_{4-x}}(d_{C-Cl})$) and the radical anion $R-Cl^{\bullet-}$ ($U_{C_2H_xCl_{3-x}+Cl^-}(d_{C-Cl})$) as a function of the C−Cl bond length,[35,37,42] where $R = C_2H_xCl_{3-x}$, as illustrated in Figure 1.

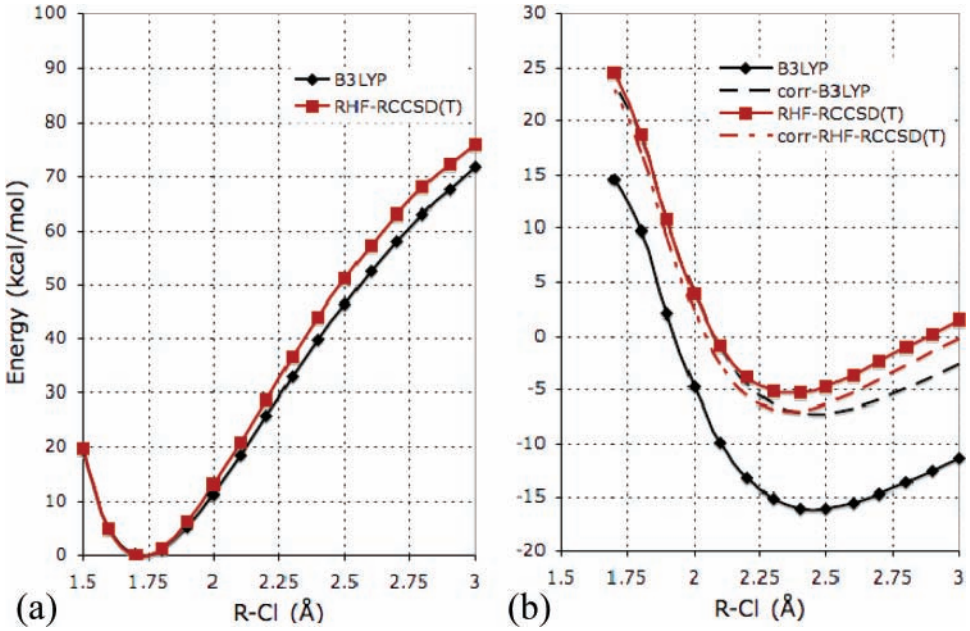

Figure 2. Gas-phase potential energy curves for (a) the neutral C_2Cl_4 and (b) the radical anion $C_2Cl_4^{\bullet-}$ calculated at B3LYP/6-311++G(2d,2p) and RHF-RCCSD(T)/aug-cc-pVTZ. The dashed lines show the corrected gas-phase potential energy curves for radical anion $C_2Cl_4^{\bullet-}$ calculated at B3LYP/6-311++G(2d,2p) and RHF-RCCSD(T)/aug-cc-pVTZ.

The solid curve is the dissociation potential energy surface for a generic C−Cl bond in chlorocarbons plus the energy of an electron in vacuum (which is set to zero). The dashed curve is the dissociative potential energy surface of the anion upon an attachment of an electron. For this reaction the anion structure is not stable and the electron transfer occurs when the neutral molecule adopts a structure close to the one at the crossing point, at which point it may capture the electron and dissociate into a chlorocarbon radical and a chloride ion. A limitation of this model is that it does not explicitly include the zero-point and entropic changes associated with the other vibrational modes besides C−Cl stretching. However, the other vibrational changes that are orthogonal to the C−Cl vibrational mode ought to be small, because the primary zero-point and entropic changes during the course of the reaction will be associated with C−Cl stretch.

The potential energy profiles ($U_{C_2H_xCl_{4-x}}(d_{C-Cl})$ and $U_{C_2H_xCl_{3-x}+Cl^-}(d_{C-Cl})$) were calculated at the ab initio levels of theory B3LYP/6-311++G(2d,2p), and RHF-RCCSD(T)/aug-cc-pVTZ//B3LYP/6-311++G(2d,2p) (i.e., RHF-CCSD(T)/aug-cc-pVTZ energies were computed at the B3LYP/6-311+G(2d,2p) optimized geometries). These curves were constructed using a series of constrained geometry optimizations, with internal coordinates, at d_{C-Cl} distances of 1.5 Å through 3.0 Å with an increment of 0.1 Å. The $U_{C_2H_xCl_{4-x}}(d_{C-Cl})$ and $U_{C_2H_xCl_{3-x}+Cl^-}(d_{C-Cl})$ data at the various ab initio levels are given as Supporting Information.

Even though the above model is simple, the ab initio theory used to calculate the potential energy curves must be chosen with care. Previous work has shown that the activation energy or "crossing point" for the concerted ET reaction in the gas phase is highly dependent on the ab initio level, and several authors have suggested that ab initio calculations with high-levels of correlation are needed to get accurate results.[35,36,57−59] An example of dissociation curves calculated at the RHF-RCCSD(T)/aug-cc-pVTZ and B3LYP/6-311++G(2d,2p) levels for the neutral and radical anion species of chloroethylene, C_2Cl_4, is shown in Figure 2. From this figure it can be seen that the level of theory does not have a significant effect on the neutral curves near the minimum (1.6−2.1 Å). The same is not true for the anion curves, because relative to the highly accurate RHF-RCCSD(T)/aug-cc-pVTZ curve the lower-level theory can be different by as much as 10 kcal/mol. Interestingly, the RHF-RCCSD(T)/aug-cc-pVTZ and B3LYP/6-311++G(2d,2p) curves for the anion parallel each other above ∼1.7 Å. This observations also applies to the other chlorinated ethylenes (not shown), which suggests that a correction scheme may be used to correct the B3LYP/6-311++G(2d,2p) curve.

Two key sources of error which could be used to correct the curves are errors in the bond dissociation energy of C−Cl bond, ΔD_e(C−Cl), and in the electron affinity of chlorine, $\Delta EA(Cl)$. The dashed lines in Figure 2 show the B3LYP/6-311++G(2d,-2p) and RHF-RCCSD(T)/aug-cc-pVTZ $C_2Cl_4^-$ anion curves with the $\Delta\chi$ correction added,

$$\Delta\chi = \Delta D_e(\text{C}-\text{Cl}) - \Delta\text{EA}(\text{Cl}) \qquad (7)$$

With this correction, where $D_e(C-Cl)_{high-level-theory}$ is estimated from results of a previous study,[21] the B3LYP/6-311++G(2d,-2p) and RHF-RCCSD(T)/aug-cc-pVTZ curves agree very well with one another. In the range between 1.7 and 2.5 Å the average absolute difference between the two corrected anion curves was 1.0 kcal/mol, and the worst case difference was found to be ∼1.7 kcal/mol at a C−Cl distance of 2.0 Å.

Our estimate of activation energies places a strong emphasis on the calculations of anion curves near the crossing point. We must point out that at C−Cl distances shorter than that of the crossing point, the anion curves are not accurate representations of the diabatic state.[34,58,60−65] These parts of the curves are shown in Figure 3 for $C_2H_3Cl^{\bullet-}$. The problem is that in the range of these shorter C−Cl distances the radical anion energy is higher that the energy of the neutral system plus a free electron, so that the radical anion preferred configuration is that of a neutral molecule plus a free electron. The bound character of the radical anion appearing to come out of the calculations is an artifact of the finite localized basis set methodology that confines the electron near the molecule. This difficulty has been previously analyzed by Bertran et al. for CH_3Cl[35] and Simons

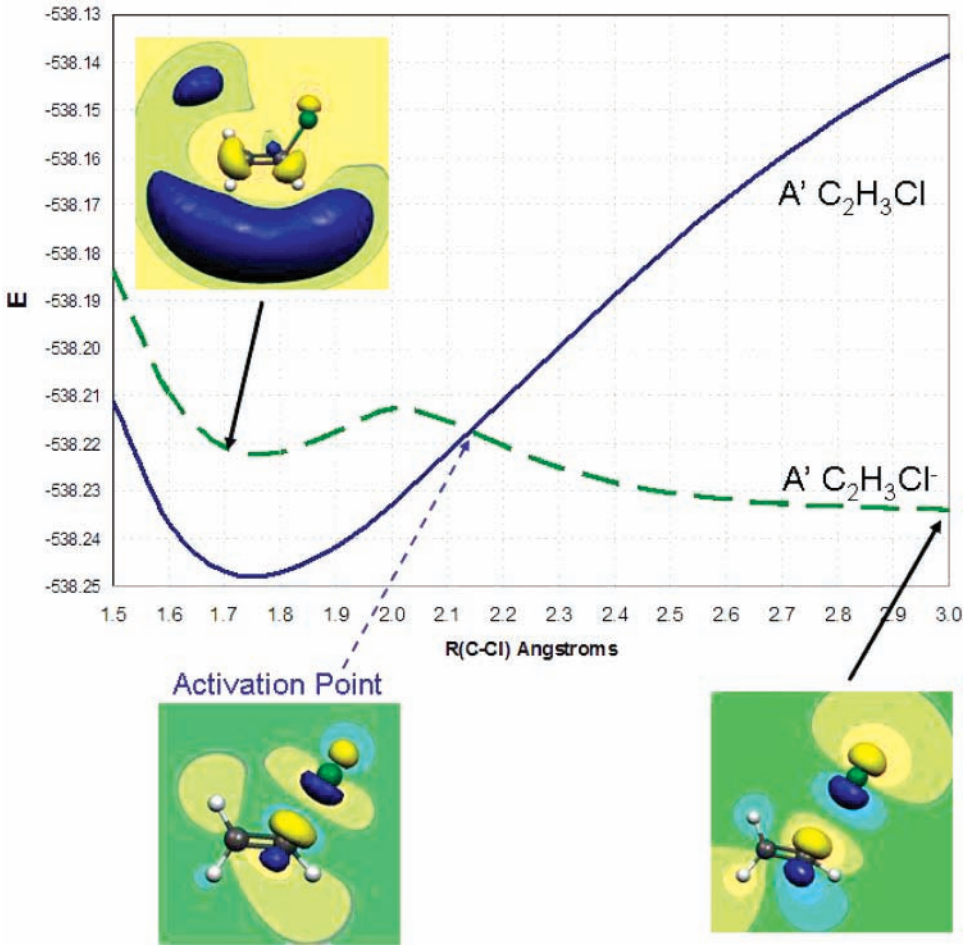

Figure 3. Highest occupied molecular orbital of the $C_2H_3Cl^{\bullet-}$ radical anion at C−Cl distances of 1.7, 2.1, and 3.0 Å. Calculations performed at the B3LYP/6-311++G(2d,2p) level.

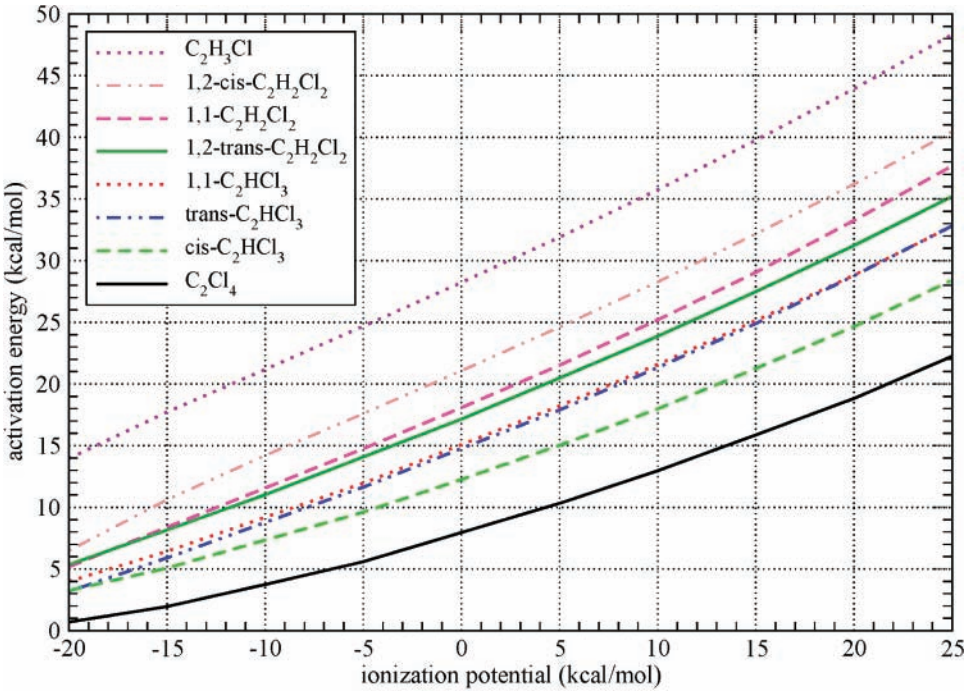

Figure 4. Activation free energies of the concerted gas-phase reactions versus the ionization potential of the reducing agent at the corrected B3LYP/6-311++G(2d,2p) level.

et al. for other radical ions.[60,65] This artifact manifested itself throughout this work whenever an anionic species had higher energy than the neutral species with the same structure. Beyond the crossing point between the neutral curve and the radical anion curve (see Figure 3) the electronic structure of the anion is completely valid insofar as the anion displays a repulsive

TABLE 1: Reaction Enthalpies, Activation Enthalpies and Activation Distances of the Gas-Phase Dissociative Electron Attachment Reactions of the Chlorinated Ethylenes versus the Ionization Potential of the Reductant at the Corrected RHF-RCCSD(T)/aug-cc-pVTZ Level

$C_2Cl_4 + e^- \rightarrow C_2Cl_3 + Cl^-$				$C_2H_3Cl + e^- \rightarrow C_2H_3 + Cl^-$			
W (eV)	E_{rxn} (kcal/mol)	E_{act} (kcal/mol)	x_{act} (Å)	W (eV)	E_{rxn} (kcal/mol)	E_{act} (kcal/mol)	x_{act} (Å)
−0.5	−7.6	2.9	1.83	−0.5	−1.9	17.6	2.09
0.0	3.9	7.7	1.92	0.0	9.6	25.5	2.20
0.5	15.4	13.5	2.01	0.5	21.2	33.9	2.30
1.0	27.0	20.6	2.10	1.0	32.7	43.1	2.43
1.5	38.5	29.0	2.20	1.5	44.2	53.2	2.58
$C_2HCl_3 + e^- \rightarrow$ *cis*-$C_2HCl_2 + Cl^-$				*cis*-$C_2H_2Cl_2 + e^- \rightarrow$ *cis*-$C_2H_2Cl + Cl^-$			
W (eV)	E_{rxn} (kcal/mol)	E_{act} (kcal/mol)	x_{act} (Å)	W (eV)	E_{rxn} (kcal/mol)	E_{act} (kcal/mol)	x_{act} (Å)
−0.5	−2.0	6.6	1.92	−0.5	1.6	13.6	2.01
0.0	9.5	12.3	2.01	0.0	13.1	21.4	2.10
0.5	21.0	19.1	2.10	0.5	24.6	29.8	2.21
1.0	32.6	27.2	2.21	1.0	36.2	39.3	2.32
1.5	44.1	36.9	2.34	1.5	47.7	49.8	2.46
$C_2HCl_3 + e^- \rightarrow$ *trans*-$C_2HCl_2 + Cl^-$				tran-$C_2H_2Cl_2 + e^- \rightarrow$ *trans*-$C_2H_2Cl + Cl^-$			
W (eV)	E_{rxn} (kcal/mol)	E_{act} (kcal/mol)	x_{act} (Å)	W (eV)	E_{rxn} (kcal/mol)	E_{act} (kcal/mol)	x_{act} (Å)
−0.5	−1.3	7.0	1.91	−0.5	1.1	10.2	1.97
0.0	10.2	14.4	2.02	0.0	12.7	18.0	2.08
0.5	21.7	22.0	2.11	0.5	24.2	25.9	2.18
1.0	33.3	30.9	2.23	1.0	35.7	34.7	2.29
1.5	44.8	41.4	2.36	1.5	47.2	44.5	2.42
$C_2HCl_3 + e^- \rightarrow$ 1,1-$C_2HCl_2 + Cl^-$				1,1-$C_2H_2Cl_2 + e^- \rightarrow$ 1,1-$C_2H_2Cl + Cl^-$			
W (eV)	E_{rxn} (kcal/mol)	E_{act} (kcal/mol)	x_{act} (Å)	W (eV)	E_{rxn} (kcal/mol)	E_{act} (kcal/mol)	x_{act} (Å)
−0.5	1.4	8.8	1.93	−0.5	−2.2	10.6	1.99
0.0	12.9	15.5	2.02	0.0	9.3	18.2	2.10
0.5	24.5	23.1	2.12	0.5	20.9	26.4	2.21
1.0	36.0	31.8	2.22	1.0	32.4	36.0	2.34
1.5	47.5	41.8	2.34	1.5	43.9	46.9	2.49

interaction with the unpaired electron of the radical species. It is also valid at shorter distances than at the crossing point, essentially all the way up to the point where the radical anion curve turns over into a local minimum with its energy higher than the energy of the neutral species. For the most part this part of the radical anion curve is not needed in the subsequent analysis. However, for extremely strong reducing agents (vide infra) this error will result in a slight underestimation of the activation barrier.

Up to this point, we have assumed the reducing agent is a free electron (i.e., has an ionization potential (IP) energy of zero). However, some ionization potential energy is required to extract an electron from most reducing agents. Reducing agents in these processes may be accommodated by including the ionization potential energy, "*W*", of the reducing agent into the curve for the neutral species, by rewriting the potential energy profiles of the products as $U_{C_2H_xCl_{3-x}+Cl^-}(d_{C-Cl}) + W$. (Similarly, one could instead rewrite the potential energy profiles of the reactants as $U_{C_2H_xCl_{4-x}}(d_{C-Cl}) - W$.) The differences in energy between the two asymptotic dissociation products are now the electron affinity of chlorine plus the ionization potential of the reductant. The more reducing the reductant, the more willing it is to give away its electron to the chlorocarbon and the more exothermic the reduction process. Decreasing the height of the anionic curve (reducing agent with negative IP) will decrease the height of the activation barrier, and conversely increasing the height of the anionic curve (reducing agent with positive IP) will increase the height of the activation barrier. In this framework, the activation barriers are then a function of ionization potential *W*, because they are determined by finding the crossing points between $U_{C_2H_xCl_{4-x}}(d_{C-Cl})$, and $U_{C_2H_xCl_{3-x}+Cl^-}(d_{C-Cl}) + W$, energy profiles.

Table 1 reports the overall reaction energy (E_{rxn}), activation barrier (E_{act}) and activation distance (x_{act}) at a variety of reducing agent ionization potentials (W) at the corrected RHF-RCCSD-(T)/aug-cc-PVTZ level. The relationship between the E_{act} and W for all the chlorinated ethylenes in the gas phase at the corrected B3LYP/6-311++G(2d,2p) level is shown Figure 4. The locations of the activated states were obtained from the (linearly extrapolated) crossing points of the energy profiles. At all levels of theory, the lowest barrier to reduction was found for the reaction

$$C_2Cl_4 + e^- \rightarrow C_2Cl_{3-x}^{\bullet} + Cl^- \qquad (8)$$

At the corrected B3LYP/6-311++G(2d,2p) level the activation barrier of this reaction varied from 0.7 kcal/mol for a −20 kcal/mol (−0.87 eV) ionization potential, to a 22.3 kcal/mol barrier for a 25 kcal/mol (1.08 eV) ionization potential. The next lowest barrier was found for the C_2HCl_3 degradation reaction

$$C_2HCl_3 + e^- \rightarrow \text{cis} - C_2HCl_2^{\bullet} + Cl^- \qquad (9)$$

At the corrected B3LYP/6-311++G(2d,2p) level, the activation barrier for this reaction varied from 3.3 kcal/mol for a −20 kcal/mol ionization potential, to a 28.4 kcal/mol barrier for a 25 kcal/

mol ionization potential. For the rest of the reactions,

$$C_2HCl_3 + e^- \rightarrow \textit{trans}\text{-}1,2\text{-}C_2HCl_2^{\bullet} + Cl^- \quad (10)$$

$$C_2HCl_3 + e^- \rightarrow 1,1 - C_2HCl_2^{\bullet} + Cl^- \quad (11)$$

$$\textit{trans} - 1,2\text{-}C_2H_2Cl_2 + e^- \rightarrow \textit{trans}\text{-}C_2H_2Cl^{\bullet} + Cl^- \quad (12)$$

$$1,1\text{-}C_2H_2Cl_2 + e^- \rightarrow 1,1\text{-}C_2H_2Cl^{\bullet} + Cl^- \quad (13)$$

$$\textit{cis}\text{-}1,2\text{-}C_2H_2Cl_2 + e^- \rightarrow \textit{cis}\text{-}C_2H_2Cl^{\bullet} + Cl^- \quad (14)$$

$$C_2H_3Cl + e^- \rightarrow C_2H_3^{\bullet} + Cl^- \quad (15)$$

the activation barriers at a −20 kcal/mol and 25 kcal/mol ionization potential were 3.2, 4.0, 5.3, 5.2, 6.5, and 14.0 kcal/mol and 32.8, 32.8, 35.2, 37.7, 40.5, and 48.3 kcal/mol, respectively.

Not surprisingly, the chlorinated ethylenes with a larger degree of chlorination are predicted to have a lower activation barrier. Somewhat more surprisingly, the reduction of C_2HCl_3 is predicted to have a significant amount of selectivity for formation of *cis*-1,2-$C_2HCl_2^{\bullet}$ over formations of the *trans*-1,2-$C_2HCl_2^{\bullet}$ and 1,1-$C_2HCl_2^{\bullet}$ radicals. This may account for the strong selectivity toward *cis*-1,2-$C_2H_2Cl_2$ seen in the solution phase measurements of C_2HCl_3 dechlorination.[5,66−69] Such a strong selectively toward *cis*-1,2-$C_2HCl_2^{\bullet}$ is remarkable given that very little difference is seen between enthalpies of formation of *cis*-1,2-$C_2HCl_2^{\bullet}$ and *trans*-1,2-$C_2HCl_2^{\bullet}$ radicals (<1 kcal/mol).[21] This suggests that the selectivity is driven by the strong tendency of the *cis*-1,2-$C_2HCl_2^{\bullet}\cdots Cl^-$ ion-dipole complex over the *trans*-1,2-$C_2HCl_2^{\bullet}\cdots Cl^-$ ion-dipole complex (∼5 kcal/mol). A significant amount of selectivity is also predicted for $C_2H_2Cl_2$. In this case, the lowest barrier is for the reduction of *trans*-1,2-$C_2H_2Cl_2$ followed by 1,1-$C_2H_2Cl_2$ and *cis*-1,2-$C_2H_2Cl_2$.

When the solvent effects are included, the energy curve for C−Cl dissociation in the neutral species is not significantly affected, whereas the anion curve is dramatically stabilized[26,46−48,58] due to the strong solvation of the anionic species Cl^-. This is expected because the charge on the anionic species strongly polarizes the solvent in contrast to a neutral molecule; e.g., the solvation energy of a chloride is −75 kcal/mol whereas the solvation energy of a chlorine atom is only 0.66 kcal/mol. However, in aqueous reduction reactions this stabilization is countered by the energy required to extract an electron from reducing species to the gas phase, because the neutral curve was generated by setting the energy of the electron to zero.

Table 2 and Figure 5 show the relationship between the activation barrier and the strength of the reducing agent for all the aqueous-phase chlorinated ethylenes at the corrected RHF-RCCSD(T)/aug-cc-pVTZ and corrected B3LYP/6-311++G(2d,-2p) levels, respectively. The ionization potential for the solvated

TABLE 2: Reaction Free Energies, Activation Free Energies and Activation Distances of the Aqueous-Phase Dissociative Electron Attachment Reaction for the Chlorinated Ethylenes versus the SHE Reduction Potential of the Reductant at the Corrected RHF-RCCSD(T)/aug-cc-pVTZ Level

$C_2Cl_4 + e^- \rightarrow C_2Cl_3 + Cl^-$

W (eV)	E_{rxn} (kcal/mol)	E_{act} (kcal/mol)	x_{act} (Å)
−2.0	−26.2	8.3	1.94
−1.5	−14.7	13.4	2.02
−1.0	−3.1	19.5	2.10
−0.5	8.4	26.9	2.21
0.0	19.9	35.5	2.34

$C_2H_3Cl + e^- \rightarrow C_2H_3 + Cl^-$

W (eV)	E_{rxn} (kcal/mol)	E_{act} (kcal/mol)	x_{act} (Å)
−2.0	−21.2	16.1	2.13
−1.5	−9.6	22.0	2.22
−1.0	1.9	28.8	2.34
−0.5	13.4	36.2	2.48
0.0	25.0	44.2	2.68

$C_2HCl_3 + e^- \rightarrow \textit{cis}\text{-}C_2HCl_2 + Cl^-$

W (eV)	E_{rxn} (kcal/mol)	E_{act} (kcal/mol)	x_{act} (Å)
−2.0	−21.2	10.6	2.00
−1.5	−9.7	16.0	2.09
−1.0	1.9	22.4	2.18
−0.5	13.4	29.8	2.31
0.0	24.9	38.4	2.46

$\textit{cis}\text{-}C_2H_2Cl_2 + e^- \rightarrow \textit{cis}\text{-}C_2H_2Cl + Cl^-$

W (eV)	E_{rxn} (kcal/mol)	E_{act} (kcal/mol)	x_{act} (Å)
−2.0	−18.7	16.1	2.07
−1.5	−7.1	22.5	2.17
−1.0	4.4	29.9	2.28
−0.5	15.9	38.1	2.40
0.0	27.5	47.0	2.57

$C_2HCl_3 + e^- \rightarrow \textit{trans}\text{-}C_2HCl_2 + Cl^-$

W (eV)	E_{rxn} (kcal/mol)	E_{act} (kcal/mol)	x_{act} (Å)
−2.0	−21.3	13.3	2.01
−1.5	−9.8	19.9	2.11
−1.0	1.7	27.3	2.22
−0.5	13.3	36.1	2.35
0.0	24.8	46.1	2.52

$\text{tran-}C_2H_2Cl_2 + e^- \rightarrow \textit{trans}\text{-}C_2H_2Cl + Cl^-$

W (eV)	E_{rxn} (kcal/mol)	E_{act} (kcal/mol)	x_{act} (Å)
−2.0	−18.7	14.9	2.07
−1.5	−7.2	21.2	2.16
−1.0	4.4	28.4	2.26
−0.5	15.9	36.4	2.39
0.0	27.4	45.3	2.54

$C_2HCl_3 + e^- \rightarrow 1,1\text{-}C_2HCl_2 + Cl^-$

W (eV)	E_{rxn} (kcal/mol)	E_{act} (kcal/mol)	x_{act} (Å)
−2.0	−17.1	14.3	2.03
−1.5	−5.5	20.7	2.11
−1.0	6.0	28.1	2.21
−0.5	17.5	36.0	2.33
0.0	29.1	45.3	2.47

$1,1\text{-}C_2H_2Cl_2 + e^- \rightarrow 1,1\text{-}C_2H_2Cl + Cl^-$

W (eV)	E_{rxn} (kcal/mol)	E_{act} (kcal/mol)	x_{act} (Å)
−2.0	−21.7	13.3	2.06
−1.5	−10.2	19.3	2.15
−1.0	1.4	26.3	2.27
−0.5	12.9	34.2	2.42
0.0	24.4	43.0	2.62

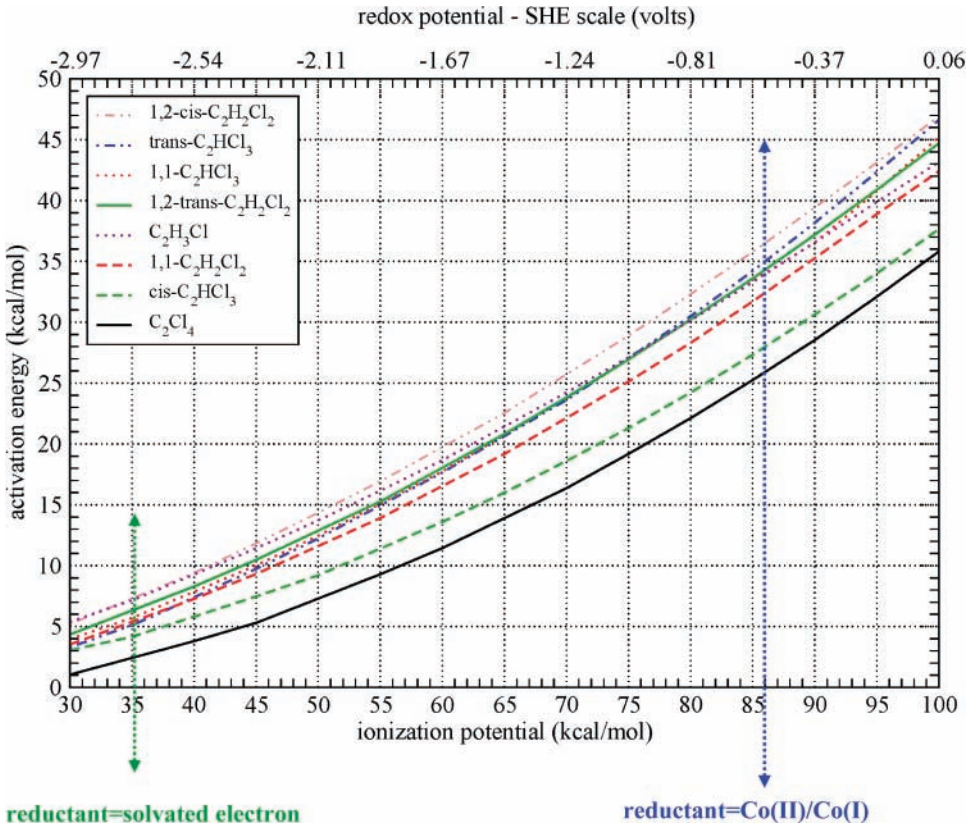

Figure 5. Activation free energies of the concerted reactions in the aqueous phase versus the ionization potential of the reducing agent at the corrected B3LYP/6-311++G(2d,2p) level. The conversion of the ionization potential to standard hydrogen electrode redox potential is shown on the top *x*-axis.

species is defined using the standard state for the COSMO solvation model, which is defined as the energy of taking an electron from the reductant in solution to the vacuum. The ionization potential is chosen to range from potentials near the strength of a solvated electron ($\Delta G_s(e^-) = -34.6$ kcal/mol[70,71]) to a standard hydrogen electrode ($E^o_H = 98.6$ kcal/mol, calculated from $\Delta G_s(H^+) = -263.98$ kcal/mol[71] and $\Delta G^o_f(H^+_{(g)}) = 362.58$ kcal/mol[72]). Typically, standard thermodynamic tables report reduction potentials in solution relative to the standard hydrogen electrode, which is defined as taking an electron from the reductant in solution to the standard hydrogen electrode. The ionization potential, *W*, can be converted to the standard hydrogen electrode redox potential simply by subtracting the true free energy of the hydrogen electrode process, $\Delta G = W - E^o_H$.

In general, solvation significantly reduced the relative activation barriers, and changed to some extent which reactions were most favorable. The relative barriers between the 8 compounds are within 5−10 kcal/mol of each other, which is down significantly from the 15−25 kcal/mol spread seen in the gas phase. The lowest activation barrier is again for reduction of C_2Cl_4, and the reduction of C_2HCl_3 is still predicted to have a significant amount of selectivity toward *cis*-1,2-$C_2HCl_2^\bullet$ over the corresponding reactions leading to the *trans*-1,2-$C_2HCl_2^\bullet$ and 1,1-$C_2HCl_2^\bullet$ radicals. More changes are seen for the chloroethylenes with higher barriers. The third lowest barrier is now for the reduction of 1,1-$C_2H_2Cl_2$ rather than other dichloro radicals found in the gas phase. This result is not entirely unexpected because the overall aqueous-phase reactive energies also predict this initial trend.[21] However, the overall ordering of the aqueous barriers is not so simply rationalized; e.g., the highest activation barrier is now for *cis*-1,2-$C_2H_2Cl_2$ rather than C_2H_3Cl.

IV. Activation Barriers for Stepwise Reaction Pathways

The activation energy for the three likely stepwise π^* reactions[21]

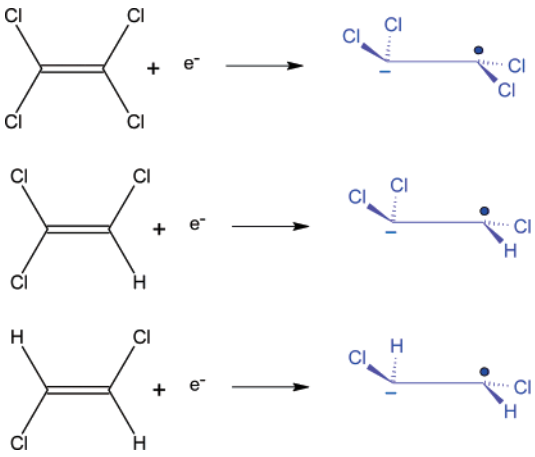

is estimated by finding the crossing point between potential energy curves for the reactants ($C_2H_xCl_{4-x} + e^-$) and the products ($C_2H_xCl_{4-x}^{\bullet -}$) as a function of the nuclear reaction coordinate. A linearized reaction coordinate, ξ, is used to define the following nuclear reaction coordinate,

$$q = (1 - \xi)q_A + \xi q_B \qquad (19)$$

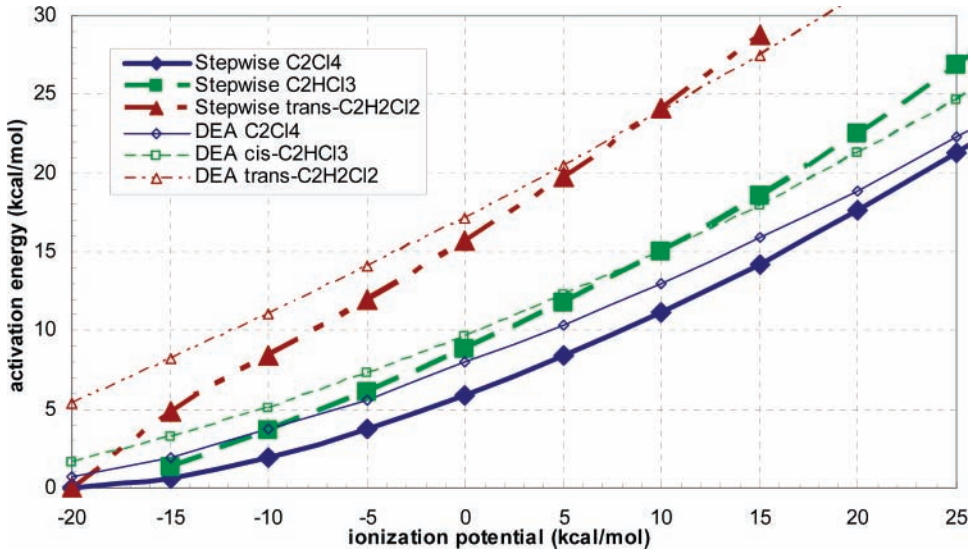

Figure 6. Activation free energies of the stepwise π^* reactions in the gas phase versus the ionization potential of the reductant at the corrected B3LYP/6-311++G(2d,2p) level. For comparisons, results are incorporated from Figure 4 for the concerted reactions involving C_2Cl_4, *cis*-C_2HCl_3, and 1,2-*trans*-$C_2H_2Cl_2$.

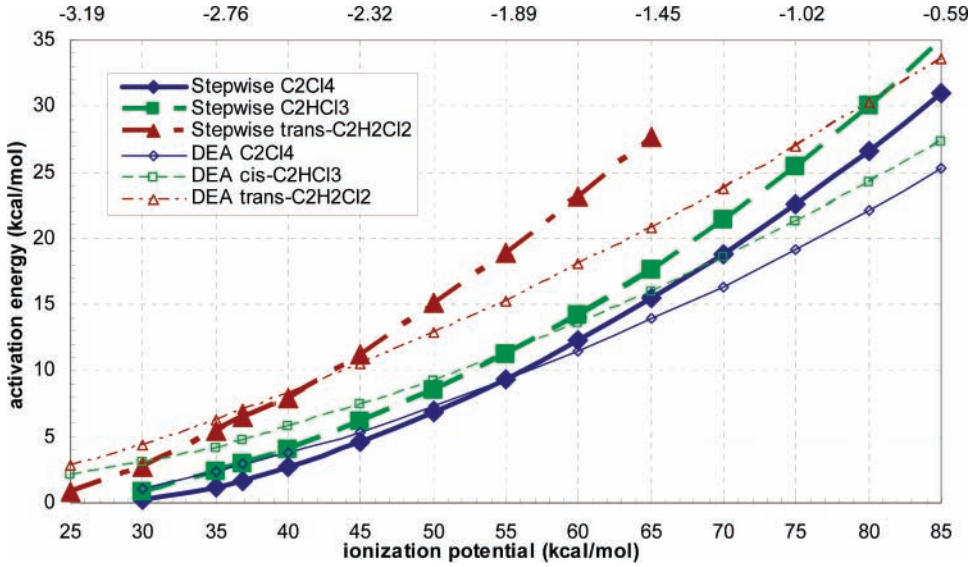

Figure 7. Activation free energies of the stepwise π^* reactions in the aqueous phase versus the ionization potential reductant at the corrected B3LYP/6-311++G(2d,2p) level. The conversion of the ionization potential to standard hydrogen electrode redox potential is shown on the top *x*-axis. For comparisons, results are incorporated from Figure 5 for the concerted reactions involving C_2Cl_4, *cis*-C_2HCl_3, and 1,2-*trans*-$C_2H_2Cl_2$.

where q_A is the optimized geometry of the neutral $C_2H_xCl_{4-x}$ and q_B is the optimized geometry of $C_2H_xCl_{4-x}^{\bullet-}$. The electron transfer occurs when the neutral molecule adopts a structure close to the one at the crossing point, at which point it captures the electron and then follows the product potential energy surface into a π^* radical anion.

The potential energy curves calculated at the B3LYP/6-311++G(2d,2p) and RHF-RCCSD(T)/aug-cc-pVTZ levels for the neutral and π^* radical anion species of chloroethylenes, C_2Cl_4, $C_2HCl_3^{\bullet-}$ and 1,2-*trans*-$C_2H_2Cl_2^{\bullet-}$ are given as Supporting Information. The level of theory does not have a significant effect on the neutral curves. The same is not true for the anion curves. However, the RHF-RCCSD(T)/aug-cc-pVTZ and B3LYP/6-311++G(2d,2p) curves parallel each other, which suggests that a correction scheme may be used to correct the B3LYP/6-311++G(2d,2p) curve. The major source of error that could be used to correct the curves is errors in the energy of the π^* radical anion. Enthalpies of formation calculated at the RHF-RCCSD(T)/aug-cc-pVTZ level are −8.45, 1.10, and 18.25 kcal/mol for the $C_2Cl_4^{\bullet-}$, $C_2HCl_3^{\bullet-}$, and 1,2-*trans*-$C_2H_2Cl_2^{\bullet-}$ π^* radical anions, respectively, and at the B3LYP/6-311++G(2d,2p) level they are −14.88, −4.30, and 14.73 kcal/mol.[21] When the B3LYP/6-311++G(2d,2p) $C_2Cl_4^{\bullet-}$ curve was corrected by $\Delta\chi = -8.45 - (-14.88) = 6.43$, the average absolute difference from the RHF-RCCSD(T)/aug-cc-pVTZ curves was found to be 0.7 kcal/mol. The worst case difference was found to be ∼2.5 kcal/mol at the linearized reaction coordinate of $\xi = 0.2$.

Figures 6 and 7 show the relationship between the activation barrier and the strength of the reducing agent for the three different stepwise reactions in the gas phase and aqueous phase at the corrected B3LYP/6-311++G(2d,2p) level. For comparisons, results are incorporated from Figures 4 and 5 for the concerted ET reactions involving C_2Cl_4, *cis*-C_2HCl_3, and 1,2-*trans*-$C_2H_2Cl_2$. These results show that for strong reducing agents the activation energy for stepwise reaction mechanism is lower than the corresponding concerted mechanism. The aqueous-phase results agree to some extent with the assertion by Costentin et al.[11] that the first ET to C_2Cl_4, C_2HCl_3, and $C_2H_2Cl_2$ proceeds via a stepwise mechanism, except that the crossover from stepwise to concerted occurs at a strong reducing

potential of ~55 kcal/mol for C_2Cl_4 and *cis*-C_2HCl_3, and ~45 kcal/mol for 1,2-*trans*-$C_2H_2Cl_2$. However, there is significant amount of uncertainty in crossover values, because the near degeneracy of these profiles, along with the uncertainty in our thermodynamic estimates, can result in large changes in the crossover value. For example, errors on the order of 2−5 kcal/mol can effect the location of the of the crossover value by as much as 30 kcal/mol.

VI. Conclusion

Ab initio electronic structures methods were used to calculate activation barriers for the reductive dechlorination of the polychlorinated ethylenes: C_2Cl_4, C_2HCl_3, *trans*-1,2-$C_2H_2Cl_2$, *cis*-1,2-$C_2H_2Cl_2$, 1,1-$C_2H_2Cl_2$, and C_2H_3Cl. Both concerted and stepwise cleavages were considered.

For concerted cleavages, the reaction barriers for the first electron reduction were estimated by using the crossing point between the energy profiles of R−Cl and $R-Cl^{\bullet-}$ as a function of the R−Cl distance. The accuracy of the activation barrier was found to be highly sensitive to the level of ab initio theory. It was found that the interaction between a radical and a closed shell anion (e.g, $R-Cl^{\bullet-}$) required high-level ab initio calculations (i.e., RHF-RCCSD(T)) to get accurate results. However, we found that the anion curve generated by lower-level B3LYP calculations parallels high-level RHF-RCCSD(T) calculations and that the accuracy of the B3LYP anion curves can be improved by correcting for the errors in the C−Cl bond dissociation energy and the electron affinity of chlorine. For this pathway, both gas-phase and aqueous-phase calculations predicted C_2Cl_4 to have the lowest reaction barrier. In addition, the reduction of C_2HCl_3 was predicted to have a significant amount of selectivity of *cis*-1,2-$C_2HCl_2^{\bullet}$ over the corresponding reactions leading to the *trans*-1,2-$C_2HCl_2^{\bullet}$ and 1,1-$C_2HCl_2^{\bullet}$ radicals and may account for the strong selectivity of *cis*-1,2-$C_2H_2Cl_2$ seen in the dechlorination of C_2HCl_3.[5,67−69]

For stepwise cleavages, the reaction barriers for the first electron reduction were estimated by finding the crossing point between potential energy curves for the reactants ($C_2H_xCl_{4-x} + e^-$) and the products ($C_2H_xCl_{4-x}^{\bullet-}$) as a function of a linearized reaction coordinate between the optimized geometry of the neutral $C_2H_xCl_{4-x}$ and the optimized geometry of π^* radical anion $C_2H_xCl_{4-x}^{\bullet-}$. As with the concerted reaction barrier calculation, the accuracy of the anion curves was found to be sensitive to the level of ab initio theory. However, the RHF-RCCSD(T) and B3LYP curves were found to parallel each other, and the accuracy of the B3LYP anion curves were improved by correcting for the errors in the energy of the π^* radical anion. It was found that for strong reduction potentials the activation energy for stepwise reaction mechanism was lower than the corresponding concerted mechanism.

Finally, a computational strategy, based on ab initio electronic structure methods and continuum solvation models that can be used to calculate the activation barriers of dissociative electron-transfer reactions of chlorinated organic compounds in solution was presented. This strategy can be used to estimate activation barriers for compounds where experimental data is unavailable, and it can be used to sort out possible reaction mechanisms for reactions that have broad relevance in environmental chemistry.

Acknowledgment. This research was supported by the Nanoscale Science, Engineering, and Technology program of the U.S. Department of Energy, Office of Science ~DE-AC06-76RLO 1830. The Pacific Northwest National Laboratory is operated by Battelle Memorial Institute. Some of the calculations were performed on the MPP2 computing system at the Molecular Science Computing Facility in the William R. Wiley Environmental Molecular Sciences Laboratory (EMSL) at PNNL. EMSL operations are supported by the DOE's Office of Biological and Environmental Research. We also thank the Scientific Computing Staff, Office of Energy Research, and the U.S. Department of Energy, for a grant of computer time at the National Energy Research Scientific Computing Center (Berkeley, CA).

Supporting Information Available: Potential energy surfaces for the concerted and stepwise pathways calculated at a variety of ab initio levels. This material is available free of charge via the Internet at http://pubs.acs.org.[73]

References and Notes

(1) Amonette, J. E.; Workman, D. J.; Kenedy, D. W.; Fruchter, J. S.; Gorby, Y. A. *Environ. Sci. Technol.* **2000**, *34*, 4606.
(2) Arnold, W. A.; Wignet, P.; Cramer, C. J. *Environ. Sci. Technol.* **2002**, *36*, 3536.
(3) Balko, B. A.; Tratnyek, P. G. *J. Phys. Chem. B* **1998**, *102*, 1459.
(4) Butler, E. C.; Hayes, K. F. *Environ. Sci. Technol.* **2000**, *34*, 422.
(5) Glod, G.; Angst, W.; Holliger, C.; Schwarzenbach, R. P. *Environ. Sci. Technol.* **1997**, *31*, 253.
(6) Li, T.; Farrell, J. *Environ. Sci. Technol.* **2001**, *35*, 3560.
(7) McCauley, K. M.; Wilson, S. R.; van der Donk, W. A. *J. Am. Chem. Soc.* **2003**, *125*, 4410.
(8) McCormick, M. L.; Adriaens, P. *Environ. Sci. Technol.* **2004**, *38*, 1045.
(9) Roberts, A. L.; Totten, L. A.; Arnold, W. A.; Burris, D. R.; Campbell, T. J. *Environ. Sci. Technol.* **1996**, *30*, 2654.
(10) Schwarzenbach, R. P.; Gschwend, P. M.; Imboden, D. M. *Environmental Organic Chemistry*; John Wiley & Sons, Inc.: New York, 1993.
(11) Costentin, C.; Robert, M.; Saveant, J. M. *J. Am. Chem. Soc.* **2003**, *125*, 10729.
(12) Pause, L.; Robert, M.; Saveant, J. M. *J. Am. Chem. Soc.* **2001**, *123*, 4886.
(13) Burrow, P. D.; Modelli, A.; Chiu, N. S.; Jordan, K. D. *Chem. Phys. Letters* **1981**, *82*, 270.
(14) Chen, E. C. M.; Wiley, J. R.; Batten, C. F.; Wentworth, W. E. *J. Phys. Chem.* **1994**, *98*, 88.
(15) Illenberger, E.; Baumgartel, H.; Suzer, S. *J. Electron Spectrosc. Relat. Phenom.* **1984**, *33*, 123.
(16) Johnson, J. P.; Christophorou, L. G.; Carter, J. G. *J. Chem. Phys.* **1977**, *67*, 2196.
(17) Kaufel, R.; Illenberger, E.; Baumgartel, H. *Chem. Phys. Lett.* **1984**, *106*, 342.
(18) Olthoff, J. K.; Tossell, J. A.; Moore, J. H. *J. Chem. Phys.* **1985**, *83*, 5627.
(19) Walter, C. W.; Smith, K. A.; Dunning, F. B. *J. Chem. Phys.* **1989**, *90*, 1652.
(20) Wiley, J. R.; Chen, E. C. M.; Wentworth, W. E. *J. Phys. Chem.* **1993**, *97*, 1256.
(21) Bylaska, E. J.; Dupuis, M.; Tratnyek, P. G. *J. Phys. Chem. A* **2005**, *109*, 5905.
(22) Nonnenberg, C.; van der Donk, W. A.; Zipse, H. *J. Phys. Chem. A* **2002**, *106*, 8708.
(23) Andrieux, C. P.; Differding, E.; Robert, M.; Saveant, J. M. *J. Am. Chem. Soc.* **1993**, *115*, 6592.
(24) Saveant, J. M. *Acc. Chem. Res.* **1993**, *26*, 455.
(25) Bylaska, E. J.; Dixon, D. A.; Felmy, A. R. *J. Phys. Chem. A* **2000**, *104*, 610.
(26) Bylaska, E. J.; Dixon, D. A.; Felmy, A. R.; Apra, E.; Windus, T. L.; Zhan, C. G.; Tratnyek, P. G. *J. Phys. Chem. A* **2004**, *108*, 5883.
(27) Bylaska, E. J.; Dixon, D. A.; Felmy, A. R.; Tratnyek, P. G. *J. Phys. Chem. A* **2002**, *106*, 11581.
(28) Bylaska, E. J. *Theor. Chem. Acc.* **2006**, *116*, 281.
(29) Borisov, Y. A.; Arcia, E. E.; Mielke, S. L.; Garrett, B. C.; Dunning, J. T. H. *J. Phys. Chem. A* **2001**, *105*, 7724.
(30) Patterson, E. V.; Cramer, C. J.; Truhlar, D. G. *J. Am. Chem. Soc.* **2001**, *123*, 2025.
(31) Winget, P.; Cramer, C. J.; Truhlar, D. G. *Theor. Chem. Acc.* **2004**, *112*, 217.
(32) Perlinger, J. A.; Venkatapathy, R.; Harrison, J. F. *J. Phys. Chem. A* **2000**, *104*, 2752.
(33) Feller, D.; Peterson, K. A.; de Jong, W. A.; Dixon, D. A. *J. Chem. Phys.* **2003**, *118*, 3510.
(34) Soriano, A.; Silla, E.; Tunon, I. *J. Chem. Phys.* **2002**, *116*, 6102.

(35) Bertran, J.; Gallardo, I.; Moreno, M.; Saveant, J. M. *J. Am. Chem. Soc.* **1992**, *114*, 9576.
(36) Tada, T.; Yoshimura, R. *J. Am. Chem. Soc.* **1992**, *114*, 1593.
(37) Pause, L.; Robert, M.; Saveant, J. M. *J. Am. Chem. Soc.* **2000**, *122*, 9829.
(38) Sun, H. Y.; Bozzelli, J. W. *J. Phys. Chem. A* **2001**, *105*, 4504.
(39) Booty, M. R.; Bozzelli, J. W.; Ho, W. P.; Magee, R. S. *Environ. Sci. Technol.* **1995**, *29*, 3059.
(40) Chen, C. J.; Wong, D.; Bozzelli, J. W. *J. Phys. Chem. A* **1998**, *102*, 4551.
(41) Sun, H. Y.; Bozzelli, J. W. *J. Phys. Chem. A* **2003**, *107*, 1018.
(42) Saveant, J. M. *J. Am. Chem. Soc.* **1987**, *109*, 6788.
(43) Hohenberg, P.; Kohn, W. *Phys. Rev. B* **1964**, *136*, B864.
(44) Watts, J. D.; Gauss, J.; Bartlett, R. J. *J. Chem. Phys.* **1993**, *98*, 8718.
(45) Kohn, W.; Sham, L. J. *Phys. Rev.* **1965**, *140*, 1133.
(46) Becke, A. D. *J. Chem. Phys.* **1993**, *98*, 5648.
(47) Lee, C. T.; Yang, W. T.; Parr, R. G. *Phys. Rev. B* **1988**, *37*, 785.
(48) Clark, T.; Chandrasekhar, J.; Spitznagel, G. W.; Schleyer, P. V. *J. Comput. Chem.* **1983**, *4*, 294.
(49) Krishnan, R.; Binkley, J. S.; Seeger, R.; Pople, J. A. *J. Chem. Phys.* **1980**, *72*, 650.
(50) Dunning, T. H. *J. Chem. Phys.* **1989**, *90*, 1007.
(51) Bylaska, E. J.; de Jong, W. A.; Kowalski, K.; Straatsma, T. P.; Valiev, M.; Wang, D.; Aprà, E.; Windus, T. L.; Hirata, S.; Hackler, M. T.; Zhao, Y.; Fan, P.-D.; Harrison, R. J.; Dupuis, M.; Smith, D. M. A.; Nieplocha, J.; Tipparaju, V.; Krishnan, M.; Auer, A. A.; Nooijen, M.; Brown, E.; Cisneros, G.; Fann, G. I.; Früchtl, H.; Garza, J.; Hirao, K.; Kendall, R.; Nichols, J. A.; Tsemekhman, K.; Wolinski, K.; Anchell, J.; Bernholdt, D.; Borowski, P.; Clark, T.; Clerc, D.; Dachsel, H.; Deegan, M.; Dyall, K.; Elwood, D.; Glendening, E.; Gutowski, M.; Hess, A.; Jaffe, J.; Johnson, B.; Ju, J.; R. Kobayashi, R.; Kutteh, R.; Lin, Z.; Littlefield, R.; Long, X.; Meng, B.; Nakajima, T.; Niu, S.; Pollack, L.; Rosing, M.; Sandrone, G.; Stave, M.; Taylor, H.; Thomas, G.; van Lenthe, J.; Wong, A.; Zhang, Z. "NWChem, A Computational Chemistry Package for Parallel Computers, Version 5.0"; Pacific Northwest National Laboratory: Richland, WA 99352-0999, 2006.
(52) Werner, H.-J.; Knowles, P. J.; Amos, R. D.; Bernhardsson, A.; Berning, A.; Celani, P.; Cooper, D. L.; Deegan, M. J. O.; Dobbyn, A. J.; Eckert, F.; Hampel, C.; Hetzer, G.; Korona, T.; Lindh, R.; Lloyd, A. W.; McNicholas, S. J.; Manby, F. R.; Meyer, W.; Mura, M. E.; Nicklass, A.; Palmieri, R.; Pitzer, R.; Rauhut, G.; Schütz, M.; Schumann, U.; Stoll, H.; Stone, A. J.; Tarroni, R.; Thorsteinsson, R. MOLPRO, a package of ab initio programs; 2002.6 ed., 2003.
(53) Tomasi, J.; Persico, M. *Chem. Rev.* **1994**, *94*, 2027.
(54) Cramer, C. J.; Truhlar, D. G. *Chem. Rev.* **1999**, *99*, 2161.
(55) Klamt, A.; Schuurmann, G. *J. Chem. Soc., Perkin Trans.* **1993**, *2*, 799.
(56) Stefanovich, E. V.; Truong, T. N. *Chem. Phys. Lett.* **1995**, *244*, 65.
(57) Eberson, L. *Acta Chem. Scand.* **1999**, *53*, 751.
(58) Piecuch, P. *J. Mol. Struct.* **1997**, *436*−*437*, 503.
(59) Roszak, S.; Koski, W. S.; Kaufman, J. J.; Balasubramanian, K. *J. Chem. Phys.* **1997**, *106*, 7709.
(60) Berdys, J.; Skurski, P.; Simons, J. *J. Phys. Chem. B* **2004**, *108*, 5800.
(61) Griffing, K. M.; Kenney, J.; Simons, J.; Jordan, K. D. *J. Chem. Phys.* **1975**, *63*, 4073.
(62) Hotokka, M.; Roos, B. O.; Eberson, L. *J. Chem. Soc., Perkin Trans.* **1986**, *2*, 1979.
(63) Luke, B. T.; Loew, G. H.; Mclean, A. D. *J. Am. Chem. Soc.* **1988**, *110*, 3396.
(64) Perez, V.; Lluch, J. M.; Bertran, J. *J. Am. Chem. Soc.* **1994**, *116*, 10117.
(65) Sobczyk, M.; Anusiewicz, W.; Berdys-Kochanska, J.; Sawicka, A.; Skurski, P.; Simons, J. *J. Phys. Chem. A* **2005**, *109*, 250.
(66) Arnold, W. A.; Roberts, A. L. *Environ. Sci. Technol.* **2000**, *34*, 1794.
(67) Burris, D. R.; Delcomyn, C. A.; Smith, M. H.; Roberts, A. L. *Environ. Sci. Technol.* **1996**, *30*, 3047.
(68) Gantzer, C. J.; Wackett, L. P. *Environ. Sci. Technol.* **1991**, *25*, 715.
(69) Shey, J.; van der Donk, W. A. *J. Am. Chem. Soc.* **2000**, *122*, 12403.
(70) Coe, J. V. *Int. Rev. Phys. Chem.* **2001**, *20*, 33.
(71) Tissandier, M. D.; Cowen, K. A.; Feng, W. Y.; Gundlach, E.; Cohen, M. H.; Earhart, A. D.; Coe, J. V.; Tuttle, T. R. *J. Phys. Chem. A* **1998**, *102*, 7787.
(72) Wagman, D. D. *J. Phys. Chem. Ref. Data* **1982**, *11*, Suppl. 2.
(73) In addition to the Supporting Information available, the optimized structures for all the molecules calculated can be obtained by correspondence with E.J.B. (Eric.Bylaska@pnl.gov).